

Optical study of hyperfine coupling in the 7F_0 and 5D_0 states of two Eu^{3+} centers in CaF_2 and CdF_2

A. J. Silversmith,* A. P. Radliński, and N. B. Manson

*Department of Solid State Physics, Research School of Physical Sciences,
Australian National University, P.O. Box 4, Canberra, Australian Capital Territory, Australia 2601*

(Received 25 July 1986)

The hyperfine interaction in the 7F_0 and 5D_0 states in oxygen-compensated Eu^{3+} centers of C_{3v} symmetry in CaF_2 and CdF_2 is reported. Optically detected nuclear-magnetic-resonance measurements determine (i) the hyperfine structure in the two states and (ii) their nuclear Zeeman splittings. In addition, optical hole burning is used to measure (iii) the quadratic electronic Zeeman effect on the ${}^7F_0 \rightarrow {}^5D_0$ transition. These three measurements associated with both ${}^{151}\text{Eu}$ and ${}^{153}\text{Eu}$ isotopes are employed to determine the magnitudes and signs of the pseudoquadrupole interactions, of the quadrupole interactions, and of the effective nuclear magnetic moments. The quadrupole interaction parameters are found to be negative in the excited state but positive in the ground state. This has been confirmed using a double-radio-frequency experimental technique. In the 5D_0 excited state the quadrupole interaction energy is dominated by the lattice contribution and is equal to -22.8 (-58.4) MHz in CaF_2 and -13.2 (33.7) MHz in CdF_2 for ${}^{151}\text{Eu}$ (${}^{153}\text{Eu}$). In the 7F_0 state there is additional contribution due to the polarization of the $4f^6$ shell equal to $+30.6$ (78.2) MHz in CaF_2 and $+20.7$ ($+53.8$) MHz in CdF_2 for ${}^{151}\text{Eu}$ (${}^{153}\text{Eu}$). The largest pseudoquadrupole contribution is for the 7F_0 state and equals 0.45 (0.33 MHz) for the case of ${}^{151}\text{Eu}$ in CaF_2 (CdF_2). The ground-state nuclear magnetic moments are only slightly affected by the $4f^6$ screening effects for the magnetic field direction parallel to the c axis of the centers. However, there is significant quenching of the nuclear magnetic moment for fields transverse to the axis: $\alpha_x = 1.85$ for CaF_2 and 1.44 for CdF_2 . This is the first time that a quenching greater than unity has been established. Matrix elements of \bar{N} and $\bar{L} + 2\bar{S}$ between the ground state and the first excited states are also determined and found to deviate as much as 60% from the value they take in the free ion.

I. INTRODUCTION

The introduction of optical hole burning and associated optical-rf double-resonance techniques has opened the possibility of detailed studies of the nuclear magnetic resonances in the Eu^{3+} system and in recent years there have been several publications in which the structure of the hyperfine levels in a magnetic field as well as in zero field have been reported. The basic theoretical background for the analysis of the data was outlined in an early work by Elliott.¹ He obtained expressions for the nuclear quadrupole and nuclear Zeeman interactions in the ground state in terms of crystal-field parameters and electronic energy-level separations. He predicted that the quadrupole interaction energy should be dominated by the second-order quadrupole polarization effect of the $4f^6$ electronic shell, whereas both the first-order lattice and the pseudoquadrupolar contributions should be small. These estimations were modified when it was realized²⁻⁴ that the core electrons could strongly amplify the effect of the lattice, resulting in the first-order interaction of the nuclear quadrupole moment, with the crystal field also becoming significant. Expressions for the various contributions to the hyperfine-interaction Hamiltonian were then given by Blok and Shirley.⁴

These predictions have been verified in a number of recent hole-burning and optically detected nuclear-magnetic-resonance (ODNMR) measurements.⁵⁻⁸ There are two naturally abundant isotopes of europium, ${}^{151}\text{Eu}$

and ${}^{153}\text{Eu}$, with different nuclear magnetic and quadrupole moments. In the 7F_0 electronic ground state the observed ratio of the quadrupole splittings associated with the two isotopes is always close to, but not equal to, the ratio of their electric quadrupole moments. This observation confirms that the magnetic pseudoquadrupole contribution is measurable but small compared with the electric quadrupole energy. Moreover, one of the electronic quadrupole contributions, namely the direct lattice term, is independent of the $4f^6$ electronic state, and yet there is usually a substantial difference between the total quadrupole interaction in the electronic ground and excited states, indicating that the remaining $4f^6$ polarization effect is of comparable magnitude. Although the relative importance of the different contributions has been well established, so far there have been few systems for which their values have been determined accurately.

In this paper the magnitudes of various contributions to the quadrupole interaction are determined for Eu^{3+} centers in CaF_2 and CdF_2 . The two electric quadrupole contributions have been discussed in an earlier paper⁸ concerned with the CaF_2 center, and in this paper the equivalent contributions for the CdF_2 center are presented. However, the major emphasis of the present work is to treat the nuclear magnetic effects as well as the pseudoquadrupole interactions. A brief account of the CaF_2 results has been given earlier.⁹

A complete determination of the several hyperfine interactions present in an axial Eu^{3+} system has been at-

tempted before for centers in $\text{LiYF}_4:\text{Eu}^{3+}$.⁷ The approach, however, necessitated substituting free-ion values for various matrix elements. For the Eu^{3+} centers studied here such approximations are not valid as some of these matrix elements depart markedly from their free-ion values. In the present work we show that there is no need to make this approximation, as Elliott's formula for pseudoquadrupole interaction can be reexpressed in terms of known constants and four experimentally determined parameters that involve the quenching of the nuclear Zeeman splitting and the magnitude of the quadratic Zeeman shift of the 7F_0 level. The earlier calculations of the pseudoquadrupole interaction also utilized information about the quenching; it is the additional incorporation of the quadratic Zeeman data that obviates the need to use an approximate value for the matrix elements. Optical hole burning provides a highly accurate means of obtaining these quadratic Zeeman shifts.

The axial Eu^{3+} centers studied were the first Eu^{3+} systems to exhibit enhanced hole burning when rf is applied at 5D_0 excited-state resonant frequencies. This enables the excited-state frequencies to be determined with much greater accuracy than can be achieved with hole-burning spectra. In addition, the quadrupole interaction in the 5D_0 state is easier to analyze than in the ground state, as the crystal-field-induced J mixing within the 5D_J multiplet is much smaller. Moreover, the pseudoquadrupole interaction is negligible there and the ratio of the corresponding quadrupole splittings associated with the ${}^{151}\text{Eu}$ and ${}^{153}\text{Eu}$ isotopes is equal to the ratio of their nuclear electric quadrupole moments. These considerations have been used in a recent work to make an accurate determination of the quadrupole moment ratio for the two Eu isotopes.¹⁰ Thus both the electric quadrupole moment and the nuclear magnetic moment ratios are known to a high degree of accuracy. For an axial center it is straightforward to determine the size of the electric quadrupole and the pseudoquadrupole contributions separately once the total interaction energy is known for the two isotopes. In the present case, we have used this information to provide a second avenue for determining the pseudoquadrupole contributions in the ground electronic 7F_0 states in both centers.

II. THE CENTERS

The two closely related sites are trigonal centers in CaF_2 and CdF_2 . The centers, denoted $G1$,¹¹ are comprised of a Eu^{3+} in a Ca^{2+} or Cd^{2+} site, charge compensated by a substitutional O^{2-} in a nearest-neighbor F^- position in the $\langle 111 \rangle$ direction. Eu-doped CaF_2 and CdF_2 crystals were grown by the Czochralski method and the oxygen centers were formed by subsequent heat treatment of these crystals. In the case of CaF_2 , heating at 800°C in an atmosphere of moist air for 8 h produced a sufficient concentration of centers and the optical quality of the crystal was not affected. Identical treatment of CdF_2 caused the crystals to turn powdery and it was found that annealing at a lower temperature of 600°C was required.

The ${}^7F_0 \rightarrow {}^5D_1$ transitions of Eu^{3+} systems are normally magnetic dipole in origin and are not changed much in

oscillator strength from site to site. Therefore, these transitions can be used to obtain a measure of the relative concentration of the various Eu^{3+} sites. In the present crystals, absorption in the appropriate wavelength region indicated that most of the Eu^{3+} ions were in the $G1$ centers. The europium concentration in both materials was 0.1 at. %, but there may be an appreciable proportion of this in the divalent state. In addition, the concentration of the $G1$ centers is not likely to be constant throughout the sample but higher near the surfaces. Nevertheless, the ODNMR frequencies and linewidths were not affected by the position of the laser beam on the crystals.

III. THEORETICAL BACKGROUND

In the absence of an external magnetic field the spin Hamiltonian describing the hyperfine coupling in the 5D_0 and 7F_0 states of an axial center is¹

$$H = (P + P')(I_z^2 - \frac{1}{3}\bar{I}^2). \quad (1)$$

The quantity P represents the electric quadrupole coupling between the nuclear quadrupole moment Q and the electric field gradient at the nucleus. This contribution is discussed in a later section.

The pseudoquadrupole coupling parameter P' is given by

$$P' = \left[\frac{2\beta\beta_N\mu_N}{I} \right]^2 \times \left[\frac{\langle r^{-3} \rangle^2 \langle 00 | N_x | 1x \rangle^2}{\Delta_{0x}} - \frac{\langle r^{-3} \rangle^2 \langle 00 | N_z | 1z \rangle^2}{\Delta_{0z}} \right], \quad (2)$$

where $2\beta_N \langle r^{-3} \rangle \bar{N}$ is an operator defined by Elliott and Stevens¹² which describes the magnetic field at the nucleus set up by the $4f$ electrons. \bar{N} produces coupling between the $J=0$ states and nearby $J=1$ states. $\langle r^{-3} \rangle$ is the average inverse cube of the distance between the $4f$ electrons and the nucleus. Δ_{0x} is the energy separation between the $J=0$ state $|00\rangle$ and the doubly degenerate $J=1$ state $|1x\rangle$ (degenerate with $|1y\rangle$), and Δ_{0z} is the separation between the $J=0$ and singularly degenerate $J=1$ state $|1z\rangle$.

Expression (2) is that obtained by a perturbation treatment using free-ion wave functions and actual energy levels. It allows for the shifts of the different hyperfine levels caused by nuclear magnetic field mixing of the ground electronic ($J=0$) and the first-excited states ($J=1$).

In a more general treatment for an $A_1 (|00\rangle)$ ground state, the expression for the effect of mixing with the first $A_2 (|1z\rangle)$ and first $E (|1x\rangle, |1y\rangle)$ excited states is unchanged, except the wave functions in (2) are eigenstates of the crystal field. For a consistent approach, however, mixing with higher A_2 and E levels should also be considered. The second A_2 level lies $\sim 1500 \text{ cm}^{-1}$ above the ground state associated with the 7F_3 state of the free ion, but as the magnetic dipole operator only couples states with $\Delta J \leq 1$, the only component of that wave function that will give field mixing will be that associated with 7F_1 . In view of the large energy denominator the resultant con-

tributions will be small. A similar situation arises in the case of the E states, with the 7F_2 $J=2$ states not being involved. The contribution from these higher-energy states can therefore be neglected and expression (2) should give a good approximation for the pseudoquadrupole interaction.

The Hamiltonian in Eq. (1) yields three doubly degenerate hyperfine levels in an $I = \frac{5}{2}$ system which are eigenstates of I and I_z . Under the influence of a weak perturbing magnetic field, the degeneracy can be lifted. The splitting is described by an effective Zeeman Hamiltonian

$$H' = \frac{\mu_N \beta_N}{I} (\bar{1} - \bar{\alpha}) \bar{B}, \quad (3)$$

which includes the first-order nuclear Zeeman term and a second-order quenching effect caused by the interaction with nearby $J=1$ levels. Elliott gave the expressions for α_i :¹

$$\alpha_i = 4\beta^2 \frac{\langle r^{-3} \rangle \langle 00 | N_i | 1i \rangle \langle 1i | L_i + 2S_i | 00 \rangle}{\Delta_{0i}}, \quad i = z, x. \quad (4)$$

In some systems, including these $G1$ centers¹³ and another axial system $\text{LiYF}_4:\text{Eu}^{3+}$,⁷ it has not been possible to determine both Δ_{0z} and Δ_{0x} for the 7F_J states. The quenching of the nuclear magnetic moment can then be used to obtain an alternative expression to Eq. (2) for the pseudoquadrupole interaction which does not contain these energy denominators:

$$P' = \left[\frac{\beta_N \mu_N}{I} \right]^2 \left[\frac{\langle r^{-3} \rangle \langle 00 | N_x | 1x \rangle \alpha_x}{\langle 00 | L_x + 2S_x | 1x \rangle} - \frac{\langle r^{-3} \rangle \langle 00 | N_z | 1z \rangle \alpha_z}{\langle 00 | L_z + 2S_z | 1z \rangle} \right]. \quad (5)$$

This is the expression given by Elliott¹ and used by Sharma and Erickson,⁷ but without substitution of the free-ion values of the matrix elements:

$$\frac{\langle 00 | N_i | 1i \rangle}{\langle 00 | L_i + 2S_i | 1i \rangle} = \frac{5/3}{2} = \frac{5}{6}. \quad (6)$$

If both matrix elements were to retain their free-ion values, then from Eq. (4) it can be seen that

$$\alpha_i \Delta_{0i} = 4\beta^2 \langle r^{-3} \rangle = 4\beta^2 (1 - R_Q) \langle r^{-3} \rangle_{\text{at}} \quad (7)$$

where R_Q is an atomic shielding factor. R_Q is small⁸ and not expected to vary much between systems. Using $\langle r^{-3} \rangle_{\text{at}} = 49.19 \times 10^{24} \text{ cm}^{-3}$,⁴ $\alpha_i \Delta_{0i}$ is expected to be within 20% of 285. For YAlO_3 the value of 286 was measured.^{5,6} However, the value for $\text{LiYF}_4:\text{Eu}^{3+}$ is 402.⁷ It will be shown that the value for CaF_2 is 401 and for CdF_2 it is 370. Clearly, for the latter three systems, there is an indication that at least one of the matrix elements for N_i and $L_i + 2S_i$ no longer retains its free-ion value.

A further magnetic effect has been analyzed in this work. This is the quadratic Zeeman shift of the ${}^7F_0 \rightarrow {}^5D_0$ transition energy. Both ground and excited $J=0$ levels are shifted to lower energy, away from the nearest $J=1$ states. The shifts to the levels are given by

$$\Delta E = -\beta^2 B^2 (M_x \sin^2 \theta + M_z \cos^2 \theta), \quad (8)$$

where

$$M_i = \frac{|\langle 00 | L_i + 2S_i | 1i \rangle|^2}{\Delta_{0i}} \quad (9)$$

and θ is the angle between the trigonal axis of the center and the magnetic field direction. The shift of the excited 5D_0 state is much smaller than that of the ground 7F_0 state and can be calculated. Hence the shift of the 7F_0 state and the values of M_z and M_x can be determined experimentally with reasonable accuracy.

By substituting in Eq. (5), a further expression for the pseudoquadrupole interaction can be obtained:

$$P' = \left[\frac{\beta_N \mu_N}{2\beta I} \right]^2 \left[\frac{\alpha_x}{M_x} - \frac{\alpha_z}{M_z} \right]. \quad (10)$$

All the constants within the first pair of large parentheses are known and all four quantities in the second pair of large parentheses are measured experimentally. Thus the pseudoquadrupole interaction can be determined without any assumptions about the values of the matrix elements of N_i and $L_i + 2S_i$.

IV. EXPERIMENTAL RESULTS FOR CaF_2 $G1$

A. Zero-field ODNMR

In the ODNMR measurements a high-resolution laser (100 mW) with a bandwidth of ~ 1 MHz was tuned in frequency to the center of the ${}^7F_0 \rightarrow {}^5D_0$ zero-phonon line at 573.6 nm. When rf was applied to a four-turn coil around the sample at a frequency corresponding to one of the ground state resonances, the emission increased due to induced hole-filling transitions.¹⁴ The hole-burning time is slow (~ 2 s) and when the spectra covering a large rf frequency range from 0 to 100 MHz were taken in a period of 100 s, the ground-state resonances gave lines with a sharp rise but slow decay. The sharp rise indicates the resonant frequency and the slow decay is due to the hole being reburned to its original depth. Differentiation of the signal using an amplifier with a cutoff frequency at 0.3 Hz gave a sharp line at the resonance position. The reburning gave a broad negative signal which should be disregarded. This general spectrum is shown in Fig. 1.

The system is axial and for each isotope there are two resonances, one at twice the frequency of the other [Eq. (1)]. Also, the positions of the resonances are approximately proportional to the nuclear quadrupole moment and hence the features associated with ${}^{153}\text{Eu}$ are about two-and-a-half times higher in frequency than the corresponding features for ${}^{151}\text{Eu}$. The positive signals are then all readily identified. In CaF_2 , ${}^{151}\text{Eu}$ has ground-state resonances at 16.52 and 33.08 MHz and ${}^{153}\text{Eu}$ resonances are at 39.85 and 79.76 MHz (Fig. 1). These precise values were determined by slow scans over a small radio-frequency range and are included in Table I with all experimentally determined parameters. The errors in the last significant figure are included in parentheses in all tables and excluded from the text.

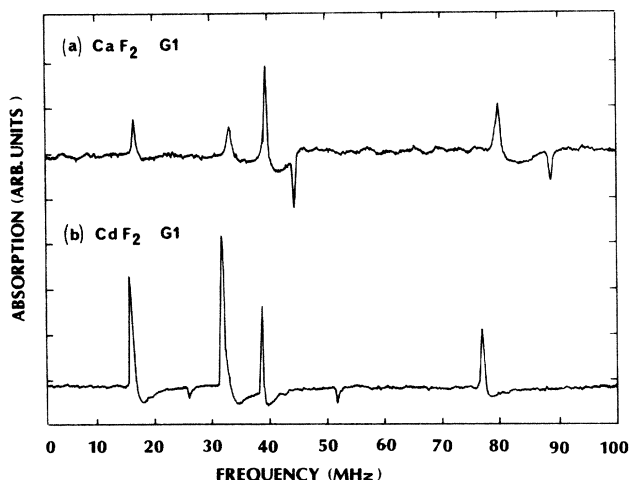


FIG. 1. ODNMR spectra in the region 0–100 MHz. (a) CaF_2 and (b) CdF_2 .

The occurrence of hole burning implies that there is some redistribution in the population arising from the optical pumping. Thus there must be some probability for the nuclear magnetic moment projection to be changed during the laser excitation or the subsequent decay. This is not expected for a truly axial system, as the nuclear quantization should be the same in the ground and excited state and there is no component in the electric dipole operator which can directly change the nuclear coordinate. Hole burning must therefore be associated with centers experiencing a small amount of nonaxial strain where $\Delta I_z = 1$ transitions are weakly allowed. In this respect it is interesting to note that when a field is applied along the z axis of a $G1$ center, no hole burning occurs. Since the I_z quantum number is now completely defined by the field and center axis, $\Delta I_z = 1$ optical transitions are strictly forbidden.

The above hole burning is of a “forbidden” nature and therefore applying a rf field at an excited-state resonance frequency to induce transitions between different I_z states can enhance the hole-burning rate. The hole becomes

deeper and, therefore, this process results in negative signals in the ODNMR spectrum. In CaF_2 , excited-state resonances are observed at 44.47 and 88.97 MHz corresponding to ${}^{151}\text{Eu}$, and at 113.7 and 227.3 MHz, corresponding to ${}^{153}\text{Eu}$.⁹ This is the first system for which excited-state Eu^{3+} ODNMR resonances have been detected. The dynamical hole burning in the excited state has a different response time than the ground state and the features exhibit marginally different linewidths from those associated with the ground state.

The ratios between the ${}^{151}\text{Eu}$ and ${}^{153}\text{Eu}$ resonances are different for the different electronic states, indicating that the pseudoquadrupole contribution must be significant in at least one of these states. Using the lower frequencies in each case the ratios are

$$39.85/16.52 = 2.412 \pm 0.005 \text{ for } {}^7F_0, \quad (11a)$$

$$113.7/44.47 = 2.556 \pm 0.005 \text{ for } {}^5D_0. \quad (11b)$$

The size of the pseudoquadrupole contribution in the 5D_0 state has been estimated in Ref. 10 using expression (2). The free-ion values are used for the matrix elements: $\langle 00 | N_x | 1x \rangle = \langle 00 | N_z | 1z \rangle = 1.36$. Other parameters are $\Delta_{0x} = 1690 \text{ cm}^{-1}$ and $\Delta_{0z} = 1828 \text{ cm}^{-1}$,¹³ and $\langle r^{-3} \rangle$ has been given earlier. The nuclear magnetic moments of ${}^{151}\text{Eu}$ and ${}^{153}\text{Eu}$ are $3.4717(6)\beta_N$ and $1.5330(8)\beta_N$.¹⁵ These yield a P' value of $3 \times 10^{-3} \text{ MHz}$ for ${}^{151}\text{Eu}$ and $6 \times 10^{-4} \text{ MHz}$ for ${}^{153}\text{Eu}$. Accepting some uncertainties of these values, it is still clear that the pseudoquadrupole contribution is less than the experimental error in determining the excited-state frequencies and hence it is negligible in that state. Thus, as presented in Ref. 10, the ratio (11b) of the resonances in the 5D_0 state corresponds to the ratio of the ${}^{153}\text{Eu}$ and ${}^{151}\text{Eu}$ quadrupole moments. It is noted that this value is different from the value of 2.67 deduced by Tanaka *et al.*¹⁶ from muonic atom data, but is in good agreement with a recent atomic-beam measurement by Brand *et al.*,¹⁷ who attained a value of 2.562. The reason for the discrepancy is not understood. The present determination, however, simply depends on the pseudoquadrupole contribution being negligible and the

TABLE I. Experimentally measured values.

Crystal	Isotope	Electronic state	Transition resonance		Zeeman splitting factor		Excitation and emission	
			$\pm \frac{1}{2} \rightarrow \pm \frac{3}{2}$ (MHz)	$\pm \frac{3}{2} \rightarrow \pm \frac{5}{2}$ (MHz)	$ 1 - \alpha_{x,y} $	$ 1 - \alpha_z $	Δ_{0x} (cm^{-1})	Δ_{0z} (cm^{-1})
CaF_2	${}^{151}\text{Eu}$	7F_0	16.52(2)	33.08(2)	0.85(2)	0.92(2)	217(1)	a
		5D_0	44.47(2)	88.97(2)	0.90(2)	0.95(2)	1690(1)	1828(1)
	${}^{153}\text{Eu}$	7F_0	39.85(2)	79.76(2)	b	b		
		5D_0	113.7(1)	227.3(1)	b	b		
CdF_2	${}^{151}\text{Eu}$	7F_0	15.7(1)	31.3(1)	0.44(2)	0.76(2)	257(1)	a
		5D_0	25.8(1)	51.5(1)	0.90(5)	0.90(5)	1732(1)	1796(1)
	${}^{153}\text{Eu}$	7F_0	38.4(1)	76.6(1)	b	b		
		5D_0	c	c				

^a 7F_1 (A_2) level not observed.

^bDetermined with low accuracy owing to small μ_N (${}^{153}\text{Eu}$), consistent with values deduced from ${}^{151}\text{Eu}$ data.

^c 5D_0 ODNMR signals not observed for CdF_2 $G1$.

Sternheimer shielding being the same (an electronic effect) for the two isotopes. The ratio of 2.556 is therefore used in later analysis. The lower ratio of 2.412 measured in the 7F_0 state, (11a), arises as a consequence of the small, but significant, pseudoquadrupole contribution.

B. ODNMR in a weak magnetic field

The splittings of the ODNMR resonances of $\text{CaF}_2:\text{Eu}^{3+}$ in an external magnetic field are shown in Fig. 2(a). The size of the splittings is reduced only marginally from that expected from the first-order nuclear Zeeman interaction $(\mu_N \beta_N / I) B_i$.

In the excited 5D_0 state the quenching α_i can be calcu-

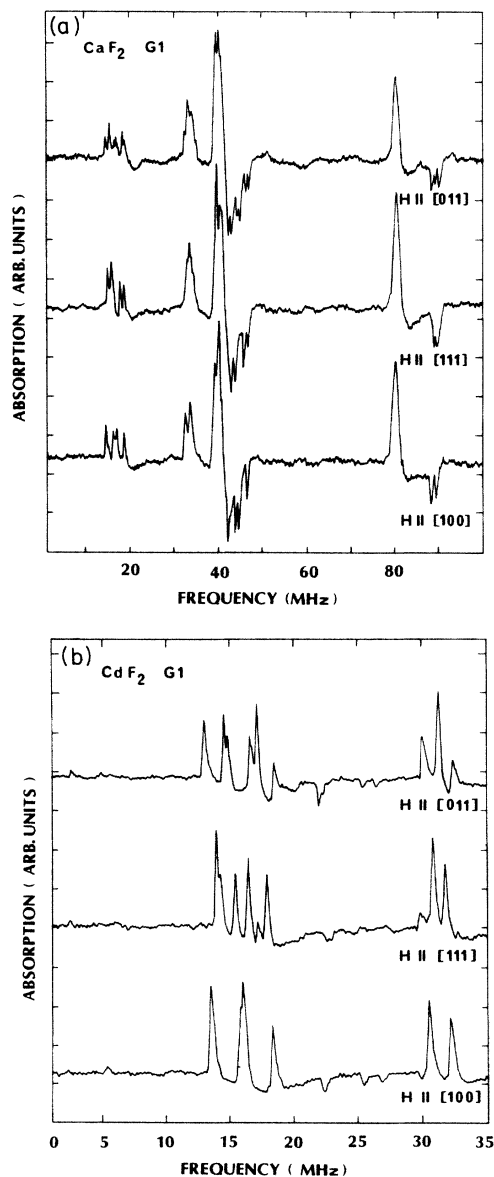


FIG. 2. ODNMR spectra in an external magnetic field oriented along the three major crystal axes. (a) CaF_2 G1, $B=1.07$ kG; (b) CdF_2 G1, $B=1.88$ kG. In the case of (b) only the ${}^{151}\text{Eu}$ resonances are shown.

lated from expression (4) to be 0.10 for the x (y) component and 0.08 for the z component. These numbers are consistent with observation.

The first impression one gets from the experimental data, in the 7F_0 state, is that the effective nuclear magnetic moment is the same as that in the 5D_0 state, as the zero-field ODNMR lines at 16.52 and 44.47 MHz are split by similar amounts. The splitting corresponds to values of $|(1-\alpha_x)|$ and $|(1-\alpha_z)|$ which are close to unity: 0.85 and 0.92, respectively (Table I). However, the sign is not determined and hence these could correspond to very small quenching of $\alpha_x=0.15$ and $\alpha_z=0.08$, respectively, or very large quenching of $\alpha_x=1.85$ and $\alpha_z=1.92$. There are therefore four different combinations of α parameters which could be substituted in Eq. (10) and these are all listed as alternative experimental values in Table III.

As noted from expression (4), the quenching is dependent on the position of the associated 7F_1 states. The 7F_1 levels are split apart from the free-ion position of 374 cm^{-1} above the ground state by a large trigonal crystal field. The doubly degenerate 7F_1 state $|1x\rangle, |1y\rangle$ lies extremely low at 217 cm^{-1} , whereas the singularly degenerate state $|1z\rangle$, although not located in emission studies, is probably considerably higher ($>600\text{ cm}^{-1}$). This is likely to lead to the α_x parameter being large and α_z being small.

C. Quadratic Zeeman shift

A hole-burning technique similar to that introduced by Macfarlane *et al.*¹⁸ was used to measure the quadratic Zeeman shift of the ${}^7F_0 \rightarrow {}^5D_0$ transition. An optical hole was burned in an external magnetic field. The field was removed and the hole spectrum scanned.

The spectrum obtained in this way is very complex as all the sideholes shift and split (Fig. 3 of Ref. 9). However, the central hole is dominated by the $\Delta I_z=0$ transitions and the hyperfine splitting is negligible compared to the quadratic shift, which can therefore be determined to within ± 10 MHz for fields up to 1 kG. Results of the experiment are summarized in Fig. 3(a) and Table II, for

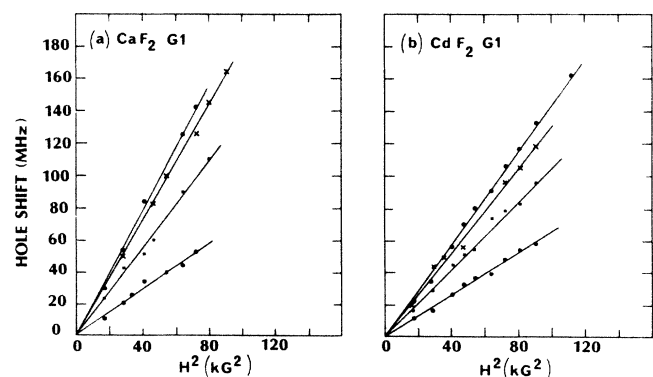


FIG. 3. Plots of the quadratic Zeeman shifts of the ${}^7F_0 \leftrightarrow {}^5D_0$ transition energy for magnetic fields along the major crystal axes (from hole-burning measurements). (a) CaF_2 G1 and (b) CdF_2 G1; solid circles— $\mathbf{B}||[110]$, solid squares— $\mathbf{B}||[100]$, and crosses— $\mathbf{B}||[111]$.

TABLE II. Quadratic Zeeman data.

θ (deg):	Observed Zeeman shift (MHz/kG ²)				
	$B \langle 110 \rangle$		$B \langle 100 \rangle$	$B \langle 111 \rangle$	
	90	36	54	72	0
CaF ₂	2.00(5)	0.72(5)	1.36(5)	1.85(5)	a
CdF ₂	1.47(5)	0.66(5)	1.07(5)	1.28(5)	a

^aNot observed.

fields along the major crystal axes. Note that there are no data with the field parallel to the major axis of the center, as no hole burning occurred in that case.

The energy shift in the 5D_0 state is given by Eq. (8) and it is calculated assuming free-ion matrix elements. Shifts of the 5D_0 level appropriate to the orientation of various centers with respect to the magnetic field are added to the observed values to obtain the 7F_0 shifts. The resultant value of the quadratic Zeeman parameters defined in Eq. (8) are $M_x = 3.2 \times 10^{-2}$ and $M_z = 2.2 \times 10^{-3}$ in units appropriate for Δ_{0x} and Δ_{0z} , cm⁻¹. The relative magnitudes are as anticipated; a large effect is observed when the relevant mixing is with the low-lying E state $|1x\rangle$ at 217 cm⁻¹, and a much smaller effect when the mixing is with the more distant A_2 state $|1z\rangle$ (at > 600 cm⁻¹).

D. Pseudoquadrupole calculation

The pseudoquadrupole interaction parameter P' can be determined by substituting the measured values of α_i and M_i in Eq. (10). The quenching parameters are more accurate for the ${}^{151}\text{Eu}$ isotope and, consequently, calculations are made for ${}^{151}\text{Eu}$ and the value of $P'({}^{153}\text{Eu})$ determined from

$$P'({}^{153}\text{Eu}) = \left(\frac{{}^{153}\mu}{{}^{151}\mu} \right)^2 P'({}^{151}\text{Eu})$$

$$= 0.195 P'({}^{151}\text{Eu}). \quad (12)$$

The four possible combinations of α_z and α_x give four values for P' for each of the isotopes (the third and fourth columns of Table III). Two give unacceptably large values of the pseudoquadrupole interactions. These correspond to cases where a large quenching factor α_z is combined with small quadratic Zeeman parameters. These are unlikely to be associated with one another as they would

correspond to large and small interaction with the $|1z\rangle$ state, respectively. A third result associated with the case of little quenching in either transverse or axial directions suggests that the size of the pseudoquadrupole interaction is negligible. This situation has already been established to be incorrect. Hence there is only one likely value of the pseudoquadrupole interaction, denoted by an asterisk in Table III, and further considerations below confirm this assertion.

The procedure to establish the correct set of parameters is for each set to subtract the pseudoquadrupole term from the total and establish the size of the electric quadrupole contribution. When this is done for both isotopes the correct set of parameters is identified as that giving a quadrupole ratio closest to 2.556.

Only the absolute values of $P + P'$ have been deduced from our ODNMR experiments. There are therefore eight possibilities to consider (Table III). The errors are substantial, but only the set marked with the asterisk gives a value of 2.54 ± 0.02 consistent with the previously determined ratio of 2.556. This set corresponds to the values of α_x and α_z and identified above with a positive sign of $P + P'$. The parameters established are summarized in Table IV.

V. EXPERIMENTAL RESULTS FOR CdF₂ G1

The same analysis has been made for the $\text{Eu}^{3+}\text{-O}^{-2}$ complex in CdF₂. The zero-field ODNMR resonances show very similar ground-state structure at 15.7 and 31.3 MHz for ${}^{151}\text{Eu}$ and 38.4 and 76.6 MHz for ${}^{153}\text{Eu}$, all being within 5% of the corresponding resonances in CaF₂ (Table I). On the other hand, the excited-state ${}^{151}\text{Eu}$ resonances are reduced to 60% of their values in CaF₂. The significance of this reduction is discussed later in Sec. VII. The excited-state resonances associated with ${}^{153}\text{Eu}$ have

TABLE III. Calculation of $P({}^{153}\text{Eu})/P({}^{151}\text{Eu})$ for all combinations of parameters.

α_z	α_x	$P'({}^{151}\text{Eu})$ (MHz)	$P'({}^{153}\text{Eu})$ (MHz)	Sign of $P + P'$	$P({}^{151}\text{Eu})$ (MHz)	$P({}^{153}\text{Eu})$ (MHz)	$\frac{P({}^{153}\text{Eu})}{P({}^{151}\text{Eu})}$
1.92(2)	1.85(2)	-6.72	-1.31	+	14.98	21.24	1.42
				-	-1.54	-18.62	12.1
0.08*(2)	1.85*(2)	0.45*(2)	0.088*(4)	+*	7.81*(1)	19.84*(1)	2.54*(2)
				-	-8.71	-20.02	2.30
1.92(2)	0.15(2)	-7.18	1.40	+	15.44	21.33	1.38
				-	1.08	-18.53	-17.2
0.08(2)	0.15(2)	-0.009	-0.002	+	8.27	19.93	2.41
				-	-8.25	-19.92	2.41

TABLE IV. Parameter values.

			α_x	α_z	M_x (10^2 cm)	M_z (10^2 cm)	$P + P'$ (MHz)	P' (MHz)	$P_{df}^{(2)}$ (MHz)	P_{lat} (MHz)
CaF ₂	¹⁵¹ Eu	⁷ F ₀	1.85(2)	0.08(2)	3.2(1)	0.22(5)	8.26(1)	0.45(2)	30.6(2)	-22.8(2)
		⁵ D ₀	0.10(5)	0.10(5)	0.12(1)	0.11(1)	-22.23(1)	< 0.01	0.6(2) ^c	-22.8(2)
	¹⁵³ Eu	⁷ F ₀	1.85(2)	0.08(2)	3.2(1)	0.22(5)	19.93(1)	0.088(4)	78.2(5)	-58.4(5)
		⁵ D ₀	0.10(5)	0.10(5)	0.12(1)	0.11(1)	-56.85(5)	< 0.01	1.6(5) ^c	-58.4(5)
CdF ₂	¹⁵¹ Eu	⁷ F ₀	1.44(2)	0.24(2)	2.41(1)	0.50(5)	7.85(5)	0.33(2)	20.7(1)	-13.2(1)
		⁵ D ₀	0.10(5)	0.10(5)	0.12(1)	0.11(1)	-12.90(5)	< 0.01	0.3(1) ^c	-13.2(1)
	¹⁵³ Eu	⁷ F ₀	1.44(2)	0.24(2)	2.47(1)	0.50(5)	19.20(5)	0.064(4)	53.8(3) ^b	-33.7(3) ^b
		⁵ D ₀	a	a	0.12(1)	0.11(1)	a	a	a	a

^aNo data.

^bCalculated using quadrupole moment ratio of 2.556.

^cEstimated to be 0.03 of P_{lat} as in Ref. 8.

not been observed and the reasons for this are not well understood, although even in CaF₂ the ⁵D₀ signals from ¹⁵³Eu are considerably weaker than those from the ¹⁵¹Eu isotope. This transition from a weak signal to no signal at all could be due to marginal changes in the nuclear-spin-relaxation rates.

The trigonal crystal field in CdF₂ is smaller than in CaF₂ and the crystal-field splittings of the ⁷F_J and ⁵D_J states are therefore reduced. The *E* state of ⁷F₁ is not as low in energy, at 257 cm⁻¹ compared with 217 cm⁻¹ in CaF₂. Again, the *A*₂ state of ⁷F₁ has not been identified, but with the smaller crystal field it must lie at lower energy than in CaF₂. The smaller splitting of the ⁷F₁ levels results in less difference between the *x* and *z* parameters (Table IV). The α_x quenching parameter is reduced from 1.85 in CaF₂ to 1.44 CdF₂, and α_z increased from 0.08 to 0.24. Similarly, the quadratic Zeeman shift parameter for the field along the transverse direction *x* is reduced from 3.2×10^{-2} to 2.37×10^{-2} and that along the *z* axis is increased from 2.2×10^{-3} to 5×10^{-3} .

The above set of parameters leads to a slightly smaller pseudoquadrupole interaction P' in the ground state: 0.33 MHz (for ¹⁵¹Eu) compared with 0.45 MHz in the CaF₂ lattice. The ¹⁵³Eu pseudoquadrupole parameter is smaller by a factor of 0.19. Following the same procedure as for CaF₂:Eu³⁺, the electric quadrupole Hamiltonian parameter P was determined. Again, it has a positive sign in the ⁷F₀ ground state. The parameters and calculated quadrupole contributions are summarized in Table IV.

VI. DEVIATION OF MATRIX ELEMENTS OF \bar{N} AND $\bar{L} + 2\bar{S}$ FROM FREE-ION VALUES

The values of the matrix elements for N_i and $L_i + 2S_i$ can be determined for the transverse field direction because the position of the ⁷F₁(*E*) state is known. In CaF₂, substitution of $\Delta_{0x} = 217$ cm⁻¹ and $M_x = 3.2 \times 10^{-2}$ in (9) yields a value for the $\langle 00 | L_x + 2S_x | 1x \rangle$ matrix element of 2.6, compared with a free-ion value of 2. In CdF₂, $\Delta_{0x} = 257$ cm⁻¹ and $M_x = 2.37 \times 10^{-2}$, and the calculated value of $\langle 00 | L_x + 2S_x | 1x \rangle$ is 2.5. Thus the deviation from the free-ion value is slightly smaller in the latter case.

Equation (4) can be used to determine the N_i matrix

elements, but it is first necessary to estimate the value of $\langle r^{-3} \rangle$. This term should be rewritten as $(1 - R_Q) \langle r^{-3} \rangle_{at}$, where $\langle r^{-3} \rangle_{at}$ is the average inverse cube of the distance between the electron and the nucleus for the free ion and R_Q is an atomic shielding factor. It has been determined for the CaF₂ G1 center that $1 - R_Q$ is very close to unity.⁸ $\langle r^{-3} \rangle_{at}$ has been given as 49.19×10^{24} cm⁻³,⁴ and using this value, $\langle 00 | N_x | 1x \rangle = 1.8$ is obtained. In view of the uncertainty in $\langle r^{-3} \rangle$, this does not indicate a significant departure from the free ion value of 1.66. Similarly, for CdF₂, a value of $\langle 00 | N_x | 1x \rangle = 1.7$ is obtained close to the free-ion value.

Estimating the sizes of the *z* component of the above matrix elements is not as straightforward because the position of the $|1z\rangle$ state has not been determined accurately. Judging from the ⁵D₁ splitting and introducing a contraction factor¹⁹ for the ⁷F₁ splittings, it must lie approximately 800 ± 200 cm⁻¹ above the ground level. The matrix element for $\langle 00 | L_z + 2S_z | 1z \rangle$ for CaF₂ is then estimated to be 1.3, a considerable decrease from the free-ion value of 2. The N_z matrix element $\langle 00 | N_z | 1z \rangle$ is also indicated to be substantially below its free-ion value (0.6 compared to 1.7). The values are summarized in Table V.

The effect of *J* mixing on the value of the calculated matrix elements has been considered, but the sizes of the changes are totally inadequate to explain the present discrepancies with the free-ion values. In attempting to explain the anomalously large transition intensities in

TABLE V. Matrix elements of \bar{N} and $\bar{L} + 2\bar{S}$ between ⁷F₀ and ⁷F₁ states.

	Free-ion value	Determined from experiment CaF ₂	CdF ₂
$\langle 00 N_x 1x \rangle$	5/3	1.8(1) ^a	1.7(1) ^a
$\langle 00 N_z 1z \rangle$		0.62(10) ^{a,b}	1.6(1) ^{a,b}
$\langle 00 L_x + 2S_x 1x \rangle$	2	2.6(1)	2.5(1)
$\langle 00 L_z + 2S_z 1z \rangle$		1.3(2) ^b	1.6(2) ^b

^aCalculated with $\langle r^{-3} \rangle = 49.19 \times 10^{24}$ cm⁻³.

^bAssuming $\Delta_{0z} = 800 \pm 200$ cm⁻¹.

these centers, other workers were similarly unable to use J mixing to account for the observed behavior and suggested that charge-transfer effects were important.²⁰ It is possible that the charge-transfer states also affect the present matrix elements, but no quantitative analyses have been attempted.

Such an approach which is based on unusually large crystal-field effects is possibly not warranted here because simple substitutional centers such as Eu^{3+} in LiYF_4 ,⁷ or isoelectronic Sm^{2+} in BaClF , also indicate departures of their matrix elements from free-ion values.¹⁸ The quadratic shifts of the ${}^7F_0 \rightarrow {}^5D_0$ transitions in Sm^{2+} in BaClF are a few percent different from those calculated with free-ion matrix elements. In $\text{LiYF}_4:\text{Eu}^{3+}$ the product of the N_i and $L_i + 2S_i$ matrix elements is 40% above that expected on the basis of free-ion computations. The reasons for the large departure from free-ion values remain unexplained, and it is highly desirable to obtain data for a system for which all the 7F_1 levels are identified and a complete crystal-field calculation can be made.

VII. ELECTRIC QUADRUPOLE TERMS FOR CaF_2 AND CdF_2

Consideration of the electric quadrupole coupling represented by the quantity P in Eq. (1) has been discussed in a recent paper⁸ and is summarized here. P can be expressed as the sum of two terms,

$$P = P_{\text{lat}} + P_{4f}^{(2)}, \quad (13)$$

where P_{lat} is proportional to the electric field gradient (EFG) set up by the lattice, multiplied by the Sternheimer antishielding factor, and $P_{4f}^{(2)}$ is due to an EFG set up by the $4f$ electrons. In general, there is also a first-order term $P_{4f}^{(1)}$ which equals zero for a (spherical) $J=0$ state. $P_{4f}^{(2)}$ is a second-order contribution due to mixing of the $J=0$ states with higher J states. Expressions for these two contributions have been given by Blok and Shirley:⁴

$$P_{\text{lat}} = -\frac{3Q}{I(2I-1)}(1-\gamma_\infty)A_{20}, \quad (14)$$

$$P_{4f}^{(2)} = \frac{6e^2Q}{I(2I-1)} \frac{A_{20}}{\Delta_2} \langle r^2 \rangle_{\text{at}} (1-\sigma_2) \times \langle r^{-3} \rangle_{\text{at}} (1-R_Q) | \langle 2||\alpha||0 \rangle |^2, \quad (15)$$

where A_{20} is the crystal-field parameter, γ_∞ the lattice Sternheimer antishielding factor, $\langle r^2 \rangle_{\text{at}} \equiv \langle 4f | r^2 | 4f \rangle$, $1-\sigma_2$ represents the change in $\langle r^2 \rangle$ in the host crystal as compared to the free ion, and the product $\langle r^{-3} \rangle (1-R_Q)$ has been defined earlier. Δ_2 is the energy distance between the ground A_1 state ($J=0$) and the A_1 ($J=2$) state. In CaF_2 , $\Delta_2 = 1219 \text{ cm}^{-1}$ and in CdF_2 , $\Delta_2 = 952 \text{ cm}^{-1}$.⁸ $\langle 2||\alpha||0 \rangle = 2/5\sqrt{3}$ is a reduced matrix element of the crystal-field potential between the $J=0$ and 2 states.

It is shown in Ref. 8 that for the 5D_0 excited state $P_{4f}^{(2)}$ can be calculated and is only a few percent of the total quadrupole coupling. Recalling that P' is also negligible in this state, this implies that P_{lat} can be obtained by subtracting the calculated $P_{4f}^{(2)}$ value. It is clear from Eq. (14) that this also gives the value in the ground state as $P_{\text{lat}}^{(2)}$ is

independent of the electronic level. As the electronic quadrupole parameter P has been determined for both 7F_0 and 5D_0 , the two contributions P_{lat} and $P_{4f}^{(2)}$ in the ground state can be derived. These are

$$P_{\text{lat}} = -22.8 \text{ MHz}, \quad P_{4f}^{(2)} = +30.6 \text{ MHz} \quad \text{for } \text{CaF}_2. \quad (16)$$

The equivalent values derived for CdF_2 are

$$P_{\text{lat}} = -13.2 \text{ MHz}, \quad P_{4f}^{(2)} = +20.7 \text{ MHz} \quad \text{for } \text{CdF}_2. \quad (17)$$

Thus it is seen that although the quadrupole parameters P in the ground states of the CaF_2 and CdF_2 systems are remarkably similar (7.81 and 7.52 MHz, respectively, for ${}^{151}\text{Eu}$), the individual terms giving rise to these are considerably different.

Crystal-field calculations have not been undertaken and thus the A_{20} values are now known, but we can make a semiquantitative self-consistency check on the validity of these values using the fact that the 5D_1 crystal-field splittings Δ are approximately proportional to A_{20} .¹⁹ The crystal-field splittings of the 5D_1 state are given in Ref. 13 and it can be seen that the following ratios are of similar size:

$$P_{\text{lat}}(\text{CdF}_2)/P_{\text{lat}}(\text{CaF}_2) = 0.58, \quad (18)$$

$$\Delta(\text{CdF}_2)/\Delta(\text{CaF}_2) = (64 \text{ cm}^{-1})/(133 \text{ cm}^{-1}) = 0.48. \quad (19)$$

In a similar way, the ratio of $P_{4f}^{(2)}$ (proportional to $A_{20}/(\Delta_2)$) is compared with the ratio of Δ/Δ_2 for the two centers:

$$P_{4f}^{(2)}(\text{CdF}_2)/P_{4f}^{(2)}(\text{CaF}_2) = 0.67, \quad (20)$$

$$[\Delta(\text{CdF}_2)/\Delta(\text{CaF}_2)][\Delta_2(\text{CaF}_2)/\Delta_2(\text{CdF}_2)] = 0.48 \times \frac{1219 \text{ cm}^{-1}}{952 \text{ cm}^{-1}} = 0.61. \quad (21)$$

In both cases the corresponding quantities are reasonably close and the differences can be explained by inaccuracies in our assumption that A_{20} is exactly proportional to Δ , as well as small differences in the shielding factors and contraction factors of the two centers.

VIII. SIGN OF THE QUADRUPOLE INTERACTION

There is no doubt that P_{lat} dominates the 5D_0 excited-state quadrupole interaction and that it has a negative sign in the excited state is not disputed. The positive sign of A_{20} in this center determines that $P_{\text{lat}} < 0$. However, we have presented calculations which predict a positive P in the 7F_0 state. It is possible to investigate whether the sign of P in the ground state is the same or reversed compared to that of the excited state by using a double-rf technique. The technique is illustrated in Fig. 4(a). Trace 1 shows the ODNMR spectrum for $\mathbf{B} || \langle 100 \rangle$. The 7F_0 and 5D_0 signals due to the $\pm \frac{3}{2} \rightarrow \pm \frac{1}{2}$ transitions are marked by arrows. Traces 2 and 3 demonstrate that the application of rf radiation at the frequency of the higher-

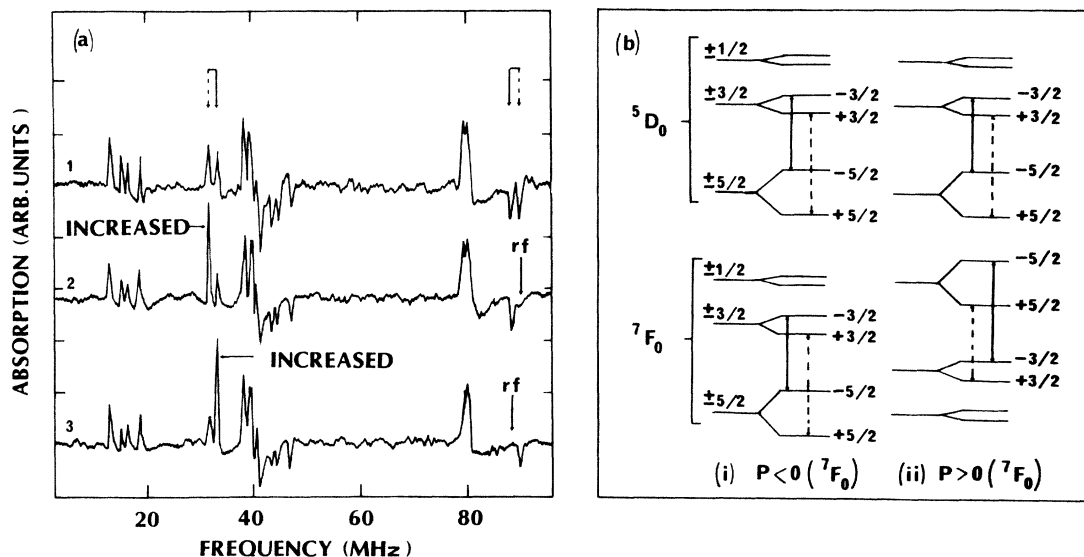


FIG. 4. (a) Double-rf measurements of CaF_2 G1 for $\mathbf{B}||[100]$. 1, ODNMR spectrum with no additional rf; 2, ODNMR spectrum recorded while rf was simultaneously applied to the sample at the frequency of the ${}^5D_0 + \frac{3}{2} \rightarrow +\frac{5}{2}$ transition, 3, ODNMR spectrum recorded while rf was simultaneously applied to the sample at the frequency of the ${}^5D_0 - \frac{3}{2} \rightarrow -\frac{5}{2}$ transition. (b) Schematic hyperfine energy-level diagrams for (i) $P({}^7F_0) > 0$ and (ii) $P({}^7F_0) < 0$. Only the ordering of levels in (ii) corresponding to $P({}^7F_0) > 0$ is consistent with the experimental results presented in (a).

energy Zeeman component of 5D_0 affects the lower-energy Zeeman component of 7F_0 . Thus, the second rf radiation applied at excited-state resonances simply helps to burn a deeper hole, thus increasing the effect of the first rf radiation at ground-state frequencies. Given that $P({}^5D_0) < 0$, the 5D_0 resonance at higher energy corresponds to the $+\frac{3}{2} \rightarrow +\frac{5}{2}$ transition [Fig. 4(b)]. The nuclear-spin projection, in general, is not changed during the decay to the electronic ground state, and hence application of rf at this frequency will affect the hole burning associated with the $+\frac{3}{2}$ and $+\frac{5}{2}$ levels in the 7F_0 state. Therefore only the right-hand energy-level scheme in Fig. 4(b), where there is a reversal of the orders of the quadrupole levels, is consistent with the experimental results. This confirms that the quadrupole structure in the CaF_2 center is reversed between the ground and excited states and therefore the quadrupole interaction parameter in the ground state is positive, with $|P_{4f}^{(2)}| > |P_{\text{lat}}|$.

Previous investigations of quadrupole interactions in Eu^{3+} systems have established a negative P term^{3,7} and $|P_{4f}^{(2)}| < |P_{\text{lat}}|$. Thus the relative value of P_{lat} and $P_{4f}^{(2)}$ must vary considerably from system to system, partly due to a variation in the shielding parameters $1 - \sigma_2$ and $1 - R_Q$. In the present systems the product of these two values is close to unity. Their values have not been established for any other Eu^{3+} system analyzed with the ODNMR technique.

IX. CONCLUDING DISCUSSION

In the excited 5D_0 state both the P' and $P_{4f}^{(2)}$ contributions to the quadrupole splitting arising from interactions within the 5D_j configuration are small. The splitting of the hyperfine levels is then dominated by the direct quadrupole term P_{lat} , which has a negative value. The

excited-state resonances observed in the ODNMR spectrum lead (with minor corrections of a few percent for the $P_{4f}^{(2)}$ contribution) to values of P_{lat} of -22.8 (-58.4) MHz in CaF_2 and -13.2 (-33.7) MHz in CdF_2 for ${}^{151}\text{Eu}$ (${}^{153}\text{Eu}$).

In the 7F_0 ground state, P' and $P_{4f}^{(2)}$ are larger, because the 7F_j levels are much closer in energy and P_{lat} remains the same as in the excited state. The total electronic quadrupole contribution $P_{\text{lat}} + P_{4f}^{(2)}$ can be separated from the pseudoquadrupole contribution by using the measured hyperfine splittings and knowledge of the ratios of the electric quadrupole moments and of the nuclear magnetic moments of the isotopes. $P_{4f}^{(2)}$ is positive in sign and is found to be slightly larger than P_{lat} . $P_{4f}^{(2)}$ is $+30.6$ (78.2) MHz in CaF_2 and 20.7 (53.8) MHz in CdF_2 for ${}^{151}\text{Eu}$ (${}^{153}\text{Eu}$). The result is a positive quadrupole interaction parameter, $P = P_{\text{lat}} + P_{4f}^{(2)}$, smaller than either P_{lat} or $P_{4f}^{(2)}$. The reversal of sign between P in the ground and excited states is confirmed independently by using a double-rf ODNMR technique.

The pseudoquadrupole term P' is smaller than both of the electric quadrupole interactions and at most is still only 6% of the resultant electric quadrupole contribution. The values of P' in the ground state are 0.45 (0.088) MHz in CaF_2 and 0.33 (0.064) MHz in CdF_2 for the ${}^{151}\text{Eu}$ (${}^{153}\text{Eu}$) isotopes.

The approach previously given by Elliott is used to establish the origin of this pseudoquadrupole interaction and obtain a further check on the above value of P' . However, when Elliott's expression for the pseudoquadrupole contribution is used directly by substitution of the observed quenching of the nuclear magnetic moment, an inconsistent value of P' is obtained. This is attributed to the approximation that the ground and first-excited states of the 7F_j multiplet are free-ion wave functions. It is con-

sidered that the free-ion wave functions do not adequately describe the actual electronic wave functions in the $G1$ center and this is supported by noting that the free-ion expressions for the quadratic Zeeman shift likewise do not predict the observed shifts. In the present work the wave functions are no longer assumed to be those of the free ion and, in particular, the matrix elements of N_i and $L_i + 2S_i$ are allowed to vary from their free-ion values. Measurements of the quenching of the nuclear magnetic moment and of the quadratic Zeeman shift are then shown to supply enough information to yield a value of P' entirely consistent with the experimental observations.

The calculated values of the matrix elements of N_i and $L_i + 2S_i$ are found to depart substantially from the values they have in a free ion. The reasons for this large departure are not well understood but assumed to be associated with the other anomalous characteristics of the $G1$ center.

The new approach is essential for overall consistency. There are also several additional attractive features about it. For example, the signs of the nuclear g values are established and it is shown that the quenching of the nuclear magnetic moment can be greater than unity. Furthermore, the treatment conclusively shows that the nuclear quadrupole contribution P in the ground state is positive.

ACKNOWLEDGMENTS

The authors would like to thank Dr. Z. Hasan for initial work in preparing and characterizing the centers, Mr. G. Sampietro for crystal growth and heat treatments, Professor H. Bill for suggesting the heat treatment of CaF_2 , and Dr. R. M. Macfarlane and Dr. G. D. Dracoulis for useful discussions. One of us (A.J.S.) would like to thank the Australian National University for financial support.

*Present address: IBM Almaden Research Center, 650 Harry Road, San Jose, California 95120-6099.

¹R. J. Elliott, Proc. R. Soc. London, Ser. B **70**, 119 (1957).

²D. T. Edmonds, Phys. Rev. Lett. **10**, 129 (1963).

³B. R. Judd, C. A. Lovejoy, and D. A. Shirley, Phys. Rev. **128**, 1733 (1961).

⁴J. Blok and D. A. Shirley, Phys. Rev. **143**, 278 (1965).

⁵R. M. Shelby and R. M. Macfarlane, Phys. Rev. Lett. **47**, 16 (1981); **47**, 1172 (1981).

⁶L. E. Erickson and K. K. Sharma, Phys. Rev. B **24**, 7 (1981); **24**, 3697 (1981).

⁷K. K. Sharma and L. E. Erickson, J. Phys. C **18**, 2935 (1985).

⁸A. P. Radliński and A. J. Silversmith, Phys. Rev. B **34**, 86 (1986).

⁹A. J. Silversmith, A. P. Radliński, and N. B. Manson, J. Phys. (Paris) Colloq. **10**, C7-531 (1985).

¹⁰A. J. Silversmith and N. B. Manson, Phys. Rev. B **34**, 4854 (1986).

¹¹F. J. Gustafson and J. C. Wright, Anal. Chem. **51**, 1762

(1979).

¹²R. J. Elliott and K. W. H. Stevens, Proc. R. Soc. London, Ser. A **218**, 553 (1953).

¹³A. J. Silversmith and A. P. Radliński, J. Phys. C **18**, 4385 (1985).

¹⁴L. E. Erickson, Opt. Commun. **21**, 147 (1977).

¹⁵L. Evans, P. G. H. Saunders, and G. K. Woodgate, Proc. R. Soc. London, Ser. A **289**, 114 (1965/66).

¹⁶Y. Tanaka and R. M. Steffen, E. B. Shara, W. Reuter, M. V. Hoehn, and Y. D. Zumbro, Phys. Rev. Lett. **51**, 1633 (1983).

¹⁷H. Brand, V. Pfeufer, and A. Steudel, Z. Phys. A **302**, 291 (1981). Values corrected for new definition of nuclear magneton as given in *Tables of Isotopes*, 7th ed., edited by C. M. Lederer and V. S. Shirley (Wiley, New York, 1978), Appendix VII, p. 56.

¹⁸R. M. Macfarlane, R. M. Shelby, and A. Winnacker, Phys. Rev. B **33**, 4207 (1986).

¹⁹B. R. Judd, Phys. Rev. Lett. **39**, 4 (1972); **39**, 242 (1977).

²⁰D. Hommel and J. M. Langer, J. Lumin. **18/19**, 281 (1979).